AMAS Workshop on Image Analysis in Investigation of Concrete
SIAIC'02 – (pp.55–63) – Warsaw, October 21-23, 2002.

Particle orientation in "natural" concrete samples from Antarctica analysed by automated and manual procedures

P. STROEVEN [1], A. P. STROEVEN [2], and J. HU [1]

[1] *Faculty of Civil Engineering and Geosciences*
Delft University of Technology
Delft, The Netherlands

[2] *Department of Physical Geography*
and Quaternary Geology
Stockholm University
Stockholm, Sweden

Nature provides deposits with a structure and properties resembling those of man-made concrete. An ancient tillite at Mt. Feather, McMurdo Dry Valleys, Transantarctic Mountains, Antarctica, is such a deposit. Stereological analysis was pursued for an objective determination of the preferred direction of small clasts in sediment samples from this deposit. This paper compares manual and automated approaches to determine the tilt angle in core samples.

1. Introduction

Tillites, like concrete, are particulate composites of which the mechanical properties are related to its structure and composition. Tillites are sedimentary rocks formed of sediments deposited by a glacier, and thereupon hardened by cementation and induration. The spatial organisation of particles in the fine-grained clayey tillite matrix are of interest to geologists because elongated particles are expected to assume a preferred direction of orientation that relates to the direction of glacier flow (in plan view) and along shear planes or micro-foliation structures. Since the horizontal reference orientation is missing, only the *tilt angle* can be determined.

Macro-fabric analysis is the traditional technique of establishing former ice flow directions in the field. This method, though widely used, is prone to operator dependent decisions on clast suitability. This problem can be largely neglected when large numbers of clasts are analysed, but this makes the procedure time-consuming and laborious. A potentially more convenient means is by micro-fabric analysis in a laboratory environment on thin sections prepared from sediment cores. The principal shortcoming of the technique is its two-dimensional character. An objective method to determine the microfabric of tillites in three dimensions is to make use of traditional *stereological* techniques such as the analysis by total projections or line scanning [1]. Stroeven *et al.* [2, 3] applied this technique to the core samples from the Sirius Group tillite on Mt. Feather, Transantarctic Mountains, Antarctica [4]. The automated and manual approaches that were adopted will be discussed in what follows. Automatic image analysis can be executed in a relatively expeditious and objective way. However, it will be shown that the relatively weak fabric of the tillite did not allow for determination of a reliable estimate by the automated procedure.

2. Modelling of tillite structure

An orthogonal set of two *vertical sections* was produced from each core sample. Smaller fields that were photographically recorded systematically probed the image plane. The material can be considered a two-phase system, consisting of a uniform matrix and dispersed non-spherical particles. The image plane indeed reveals the typical features of such a structure (Fig. 1). For visualisation purposes the particles can be assumed oblong (primarily elongated in one direction), or oblate (primarily elongated in two directions). For a system of such particles with a preferred orientation, the orientation axis, l,

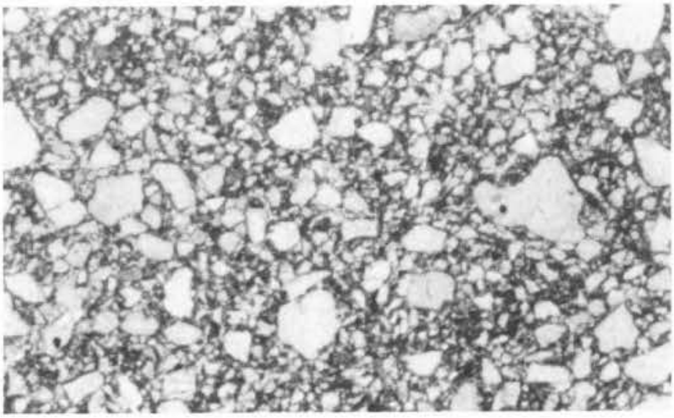

Figure 1. Example of field image (36×24 mm).

and the xy-plane of a Cartesian coordinate system $\{x, y, z\}$ enclose the *tilt angle* α (Fig. 2). The xy-plane is called the horizontal plane, because it approximately corresponds to a plane perpendicular to the earth's radius at the original core location. The two vertical sections, used for the investigations, are defined by the xz-plane and the yz-plane, respectively. Photographs of (part of) the image planes were subjected to a directed secants analysis for the construction of roses-of-intersections, from which the respective angles of preferred orientation in the plane, β and γ, can be derived (Fig. 2). The tilt angle is given by

$$\tan^2 \alpha = \tan^2 \beta + \tan^2 \gamma. \tag{2.1}$$

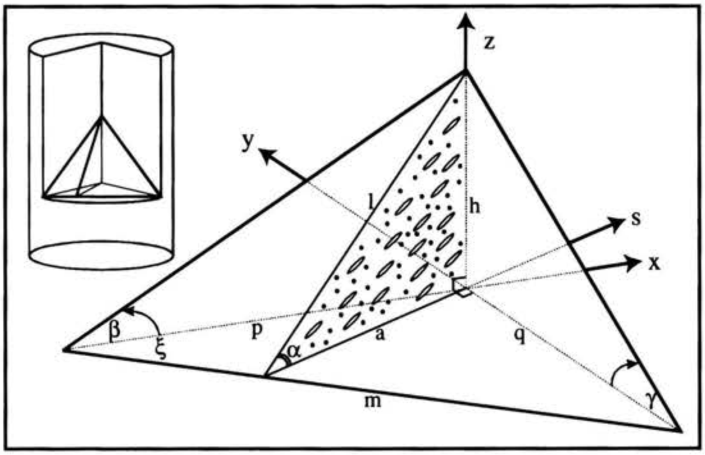

FIGURE 2. Tilt angle α and angles of preferred orientation β and γ in vertical sections $\{x, z\}$ and $\{y, z\}$, respectively.

3. Orientation analysis by line scanning

The number of intersections in the directed secants analysis is indicated by P, and the intersection density by $P/L = P_L$, where L is the total line length of the grid. Perpendicular to the orientation axis of the traces the intersection density will have a maximum, while a minimum is found parallel to the orientation axis. It is well known that the intersection density in a certain direction, $P_L(\theta)$ will equal the total projected length of the traces (L') per unit of area (A), on a line perpendicular to the grid direction, $L'_A(\theta + \pi/2)$ [5]. Basically, the method of total projections yields qualitatively similar information and could have been selected as well for the orientation analysis.

For the two-dimensional case, it is assumed that the actual trace system can be approximated by a mixture of random and oriented line segments, respectively L_r and L_o. L_o is considerably smaller than L_r in the present case. By dividing by the sampled area, A, the appropriate line densities are obtained. This allows constructing a rose of intersections for a system of random and oriented line segments in a vertical plane, of which the latter enclose an angle $\beta + \pi/2$ with the horizontal (say, x-) axis. This type of approach has been applied in concrete technology to analyse crack density and orientation [6, 7]. In the case of the digitised image, all line segments building up the particle's perimeter in the section plane are replaced by their total projections in the x- and y-directions.

3.1. Rose for partially oriented system of line segments in a plane (manual model)

The contours of the particles are smooth in the analogue picture subjected to the manual orientation analysis. It is assumed that in the orthogonal pair of vertical sections these perimeter traces can be conceived as a mixture of 2-D randomly oriented segments and oriented ones. The treatment is similar for the two vertical sections, so that the discussion can be restricted to the xz-plane only. The number of intersections per unit of line length is on average

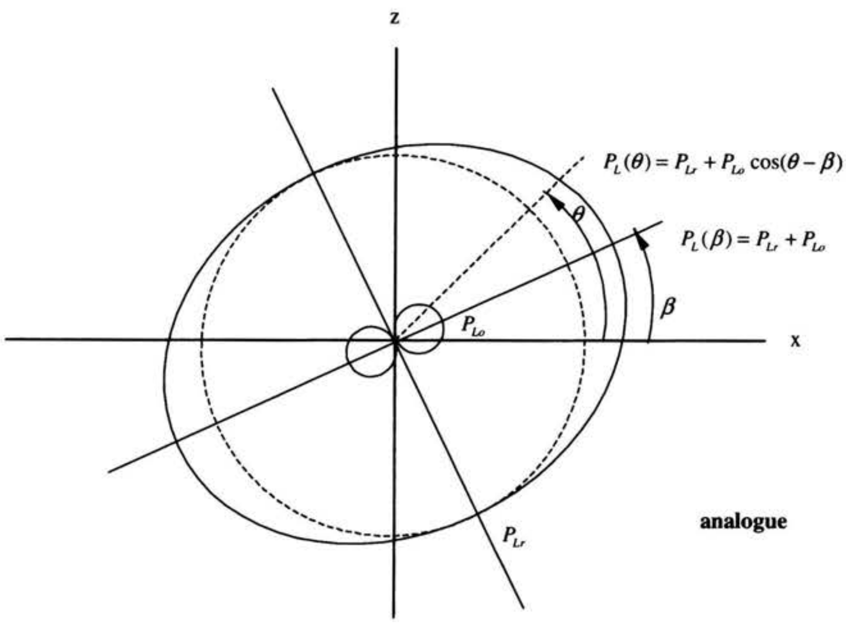

FIGURE 3. Rose of intersections for a combination of 2-D random and oriented line segments, the latter enclosing an angle of preferred orientation β with the x-axis.

a constant for the random portion of line segments, say $P_{L\mathrm{r}}$. The oriented portion reveals a maximum value, $P_{L\mathrm{o}}$, perpendicular to the direction of preferred orientation, in a direction enclosing an angle β with the x-axis. The value will decline when the line system is rotated over an angle θ to $P_{L\mathrm{o}}\cos\theta$. These two components are combined in Fig. 3 (c.f. Fig. 3.8 in [5]). The large circle, with radius $P_{L\mathrm{r}}$, represents the random portion. The two smaller circles pass through the origin; they have a diameter $P_{L\mathrm{o}}$, while the line through their centres (and the origin) encloses an angle β with the x-axis. Hence, $P_L(\theta)$ would be given by

$$P_L(\theta) = P_{L\mathrm{r}} + P_{L\mathrm{o}}\cos(\theta - \beta). \tag{3.1}$$

This rose has its maximum value of $P_L(\theta)$ for $\theta = \beta$ with $P_{L\max} = P_{L\mathrm{r}} + P_{L\mathrm{o}}$. Note that Eq. (3.1) will also hold for the number of intersections when L is a constant (as in our investigations).

3.2. Rose for mixture of orthogonal systems of line segments in a plane (automated model)

The perimeter contours in the digitised images are composed of orthogonal line segments due to digitisation in 4-connexity. They are oriented in either the x- and z-directions, or in the y- and z-directions, respectively. Because of similarity, the discussion can be restricted to the xz-plane only. The oriented portions are represented by circles passing through the origin and oriented in x- and z-directions, respectively (Fig. 4). The diameter of the vertical pair of circles is denoted by $P_L(\pi/2)$, whereas the diameter of the horizontal pair of circles is $P_L(0)$. Since $P_L(\theta) = P_L(0)|\cos\theta| + P_L(\pi/2)|\sin\theta|$ in the four quadrants, it can be derived that $P_L(\theta)$ will have its maximum value for $\tan\beta = P_L(\pi/2)/P_L(0)$. Upon substitution, the expression for intersection density in an arbitrary direction θ $(0 \leqslant \theta \leqslant \pi)$ is found:

$$P_L(\theta) = \frac{P_L(0)}{|\cos\beta|}\left|\cos(\beta - \theta)\right|. \tag{3.2}$$

Comparing Eqs. (3.1) and (3.2) reveals that the two representations of the *same image* are different on important aspects, as reflected by Figs. 3 and 4. Figure 3 is symmetric around an orthogonal system of axes, inclined by an angle β with the x-axis. Figure 4 is symmetric around x- and z-axes (c.f. Fig. 3.3(b-2) in [5]). In Fig. 3, the shape of the curve in the two successive quadrants is different; in Fig. 4 they are similar, with the crucial consequence of not being able to determine whether the preferred orientation of the clasts is in a direction β or in a direction π-β! Selection of the proper solution

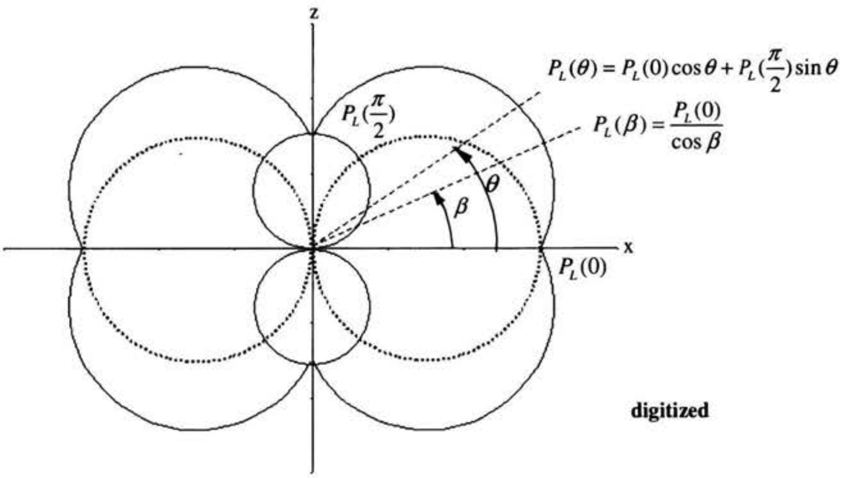

FIGURE 4. Rose of intersections for an orthogonal set of oriented line segments in x- and z-directions, respectively.

between these two options should be based on insight into the technical problem. Basically, in both situations the angle β can be obtained by fitting a cosine function to the data set.

4. Experimental verification

Images of probe areas with a size of 36×24 mm were available for the *automated* analysis. For further elaboration, the scanned (digitised) images (at 820×520 pp resolution) were employed. Specifically, 13 defect-free 340×340 pp square probe areas per vertical section were used for further analysis. All probe images with linear dimensions of about 15 mm were subjected to a software-driven filtering operation, leading to a particulate structure from which the fines were removed. The fields were subjected to the directed secants analysis. All particle sections having the tangent point with a horizontal line at the bottom side of its perimeter outside the field were omitted from the orientation analysis. The probe areas were projected with a magnification of about $20\times$ on a semi-transparent screen and manually copied for the *manual* analysis. Only sand-sized particles in the section image were admitted. These field images were subjected manually to a directed secants analysis by superimposing a grid engraved on a circular Perspex plate of 300 mm diameter. The grid consisted of equidistant grid lines 10 mm apart. This line spacing offered optimum counting statistics.

(a)

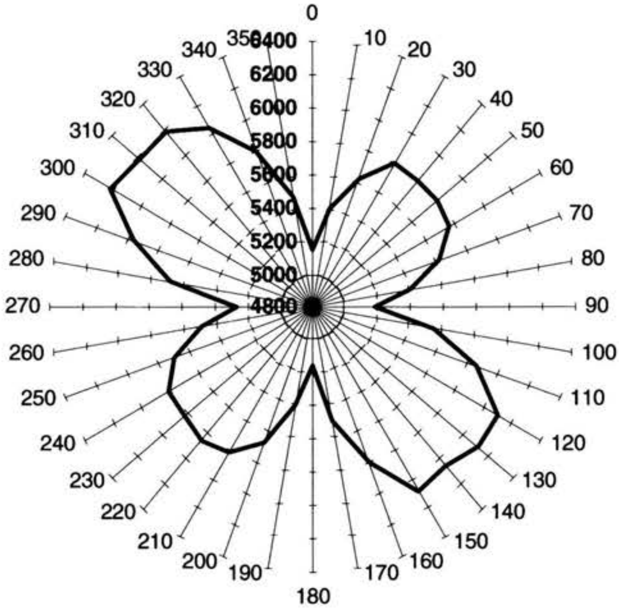

(b)

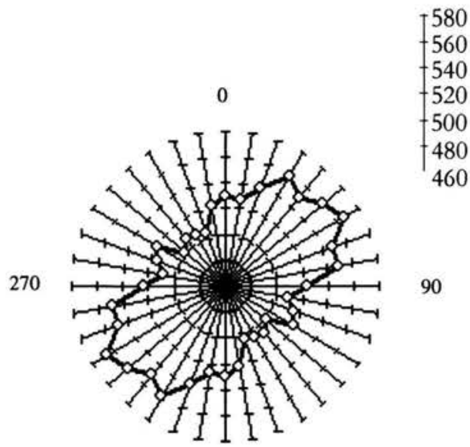

FIGURE 5. Flower-shaped rose of intersections of single probe area subjected to automated image analysis approach (a); rose of intersections with preferred orientation of single probe area obtained by manual image analysis approach (b). Probe areas are representative for the two sets of 13 fields per vertical section of cores drawn from an Antarctic tillite.

In all cases, roses pertaining to a particular vertical section were combined to yield an average (automated procedure) or total (manual procedure) rose-of-intersections. The amount of scatter was reduced as a result in these roses. The roses in the automated procedure (see Fig. 5(a)) had flower-like shapes in agreement with the model displayed in Fig. 4. All the individual roses obtained by the manual procedure of image analysis clearly revealed a direction of preferred orientation (see Fig. 5(b)). For data and elaboration of the tilt angle, see the relevant literature.

5. Discussion

The flower-like shape of roses for which Fig. 5(a) is representative demonstrates that the digitisation effect hampers reliable assessment of the angle of preferred orientation in the automated approach. This is due to the weak fabric. This can be improved by digitisation by higher order digitisation lattices.

6. Conclusions

The presented stereological approach to three-dimensional orientation analysis for determination of the tilt angle of small clasts in Antarctic tillite is objective and exact, and can be automated. A similar approach is possible in case of man-made concrete where a preferred orientation of particles may be due to a particular compaction technique, or where crack orientation is of interest [6, 7].

An accurate estimate of the direction of the main axes of the rose of intersections is derived by the method of directed secants, even when analysing weak orientation signals as in the present problem. Determination by manual procedure on analogue images results in a straightforward analysis, when combined with a cosine function curve fitting operation.

The effect of digitisation on roses of intersections of the automatic image analysis hampers the determination of a reliable estimate for the preferred orientation in the vertical sections [2, 3]. This well-known disturbing effect [8] can be somewhat reduced by subjecting fields of larger magnification to the directed secants analysis and using 6- or 8-connexity digitisation lattices.

References

1. D. STOYAN, V. BENES, Anisotropy analysis for particle systems, *Journal of Microscopy*, Vol.164, pp.159-169, 1991.

2. P. STROEVEN, A.P. STROEVEN, D.H. DALHUISEN, J. VAN DER MEER, Stereological Analysis of ice flow-induced preferred orientation of small clasts in Tertiary tillite matrix of Mt. Feather, *Acta Stereologica*, Vol.18/1, pp.49-60, 1999.

3. P. STROEVEN, A.P. STROEVEN, D.H. DALHUISEN, Image Analysis of "natural" concrete samples by automated and manual procedures, *Cement and Concrete Composites*, Vol.23, pp.227-236, 2001.

4. A.P. STROEVEN, J. KLEMAN, Age of Sirius Group on Mount Feather, McMurdo Dry Valleys, Antarctica, based on glaciological inferences from the overridden mountain range of Scandinavia, *Global and Planetary Change*, Vol.23(1-4), pp.231-247, 1999.

5. E.E. UNDERWOOD, *Quantitative Stereology*, Addison-Wesley Publ Co Reading (Ma), 1970.

6. E. RINGOT, Automatic quantification of microcracks network by stereological method of total projections in mortars and concrete, *Cement and Concrete Research*, Vol.18, pp.35-43, 1988.

7. P. STROEVEN, Geometric probability approach to the examination of microcracking in plain concrete, *Journal of Materials Science*, Vol.14, pp.1141-1151, 1979.

8. J.M. CHAIX, F. GRILLON, On the rose of directions measurements on the discrete grid of an automatic image analyser, *Journal of Microscopy*, Vol.184, pp.208-213, 1996.